

1 Effect of copper addition on the cluster formation behavior of Al-Mg-Si,
2 Al-Zn-Mg and Al-Mg-Ge in the natural aging

3
4 DAICHI HATAKEYAMA, KATSUHIKO NISHIMURA, KENJI MATSUDA, TAKAHIRO
5 NAMIKI, SEUNGWON LEE, NORIO NUNOMURA, TETSUO AIDA, TEIICHIRO
6 MATSUZAKI, RANDI HOLMESTAD, SIGURD WENNER, and CALIN D. MARIOARA

7
8
9 DAICHI HATAKEYAMA, KATSUHIKO NISHIMURA, KENJI MATSUDA, TAKAHIRO
10 NAMIKI, SEUNGWON LEE, NORIO NUNOMURA, and TETSUO AIDA are with the Graduate
11 School of Science and Engineering, University of Toyama, Gofuku, Toyama, 930-8555, Japan
12 TEIICHIRO MATSUZAKI is with RIKEN Nishina Center for Accelerator Based Science, RIKEN,
13 Wako, Saitama 351-0198, Japan
14 RANDI HOLMESTAD is with the Department of Physics, NTNU, Høgskoleringen 5, Trondheim
15 NO-7491, Norway
16 SIGURD WENNER and CALIN D. MARIOARA are with the Materials and Chemistry SINTEF,
17 Høgskoleringen 5, Trondheim NO-7491, Norway

18
19 *Corresponding author, E-mail: nishi@eng.u-toyama.ac.jp
20

1
2
3
4
5
6
7
8
9
10
11
12
13
14
15
16

Abstract

The time dependent resistivity of Al-Mg-Si(-Cu), Al-Zn-Mg(-Cu) and Al-Mg-Ge(-Cu) alloys are studied over a range of constant temperatures between 255 and 320 K. The resistivity vs. time curves for the samples show three temperature stages associated with solute element-vacancy clustering. Cu addition was found to make the stage transition time longer for the studied samples. Arrhenius plots of the transition time vs. temperature provide the activation energy (Q) of clustering from stage I to II and stage II to III. While the Cu addition increased the Q (I-II) values of Al-1.0%Mg₂Si-0.20%Cu and Al-2.68%Zn-3.20%Mg-0.20%Cu, it was found that the added Cu decreased the Q (I-II) value of Al-0.44%Mg-0.19Ge-0.18%Cu. The Q (II-III) values of Al-1.0%Mg₂Si and Al-2.68%Zn-3.20%Mg were slightly decreased by the Cu addition. The different effect of added Cu on the Q values is discussed in terms of diffusivity and binding energy between vacancies and solute elements.

Keywords: time dependent resistivity, Cu addition effect, clustering reaction, activation energy

1
2
3
4
5
6
7
8
9
10
11
12
13
14
15
16
17
18
19
20
21
22
23
24
25
26
27
28
29
30
31
32
33
34

1. Introduction

It is well known that the mechanical hardness of Al-Mg-Si (6xxx series) [1] and Al-Zn-Mg (7xxx series) [2] alloys are strongly related to microstructure and number densities of solute element precipitates, which are formed during natural aging (NA) and artificial aging (AA) after solution heat treatment (SHT) followed by a quick quench in water (SHTQ). The microstructure of the precipitates has been intensively studied via transmission electron microscopy (TEM) [3-6] and atom probe tomography (APT) [7-12] to reveal the age hardening mechanism. Differential scanning calorimetry (DSC) [13-15] has been widely used to investigate cluster formations and precipitation processes. Positron annihilation lifetime spectroscopy (PALS) [16-18] and muon spin relaxation spectroscopy (μ SR) [19-21] have been used to investigate the vacancy and clustering behavior. Despite these studies, the precipitation processes, especially the early stages of clustering at NA, are still not fully understood. Recent comprehensive reviews [1, 22] of solute and trace element effects on the natural aging phenomena suggest that there are at least five stages of clustering at NA in the Al-Mg-Si alloys. After SHT and quenching, within a few minutes there are plenty of free excess vacancies (stage 0), but it has been quite difficult to obtain reliable data to confirm this stage. In the next stage (stage I), solute-vacancy pairs start to form and build up to solute-complexes at the end of this stage; solute-rich clusters in stage II and solute co-clusters, such as Si-Mg clusters, in stage III are expected to form. NA time evolutions of mechanical hardness and electrical resistivity from the stage I to III have been well correlated with PALS and/or DSC observations [22, 23]. In stage IV, coarse or ordered clusters possible emerge, often observed by APT. The complexity of the precipitation process is due to significant sensitivity of solute clustering kinetics to the solute/trace element concentrations and NA temperatures, which dominate the duration and activation energy of each stage [1].

In the early stages of clustering, vacancies are considered to play an important role. It has been frequently observed that Cu addition to Al-Mg-Si delayed the Si/Mg-vacancy pairing and Si-complex/cluster formation (stage I) [10, 24, 25], implying that Cu has a relatively larger binding energy with vacancies in aluminum, and thus it is difficult for solute Si and Mg to cluster and bind to vacancies. In this paper, the effect of Cu addition on the activation energy for cluster formation in Al-Mg-Si(-Cu), Al-Zn-Mg(-Cu) and Al-Mg-Ge(-Cu) alloys is reported via electrical resistivity measurements. The findings are discussed by considering the diffusivity of solute elements and Cu-vacancy binding energy.

2. Experimental Procedure

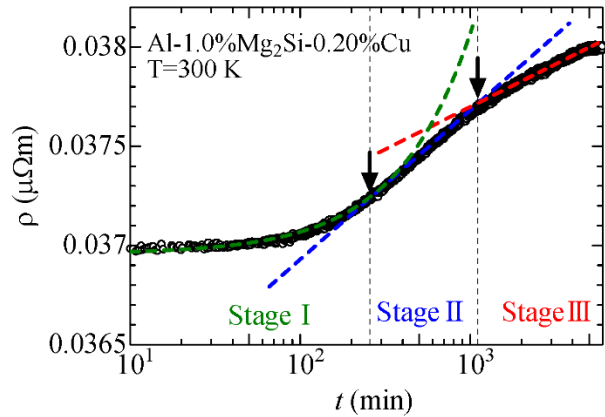
The materials used in this study were prepared by melting pure Al (purity, 99.99 %) with Si and

1 Mg (purity, 99.9 %), Cu and Zn (purity, 99.99 %) in air. The resulting ingots were formed into 2.0
2 mm thick plates by hot and cold rolling. Several pieces of the samples were cut out from the plate
3 with the approximate dimensions of $1.0 \times 2.0 \times 30.0 \text{ mm}^3$. The chemical compositions, sample
4 notations, and heat treatment temperatures are described in Table 1. No oxidation products, such
5 MgO or SiO₂, were noticed on a scanning electron microscope (SEM), X-ray diffraction, and TEM
6 [5] observations. Four Pt wires were welded on the samples for resistivity measurements. The
7 samples were annealed at 848/753/873 K for 1 hour solution heat treatment and directly quenched
8 into ice-water. The samples were set on the sample holder of an electrical resistivity measurement
9 system within five minutes after quenching. The time dependent resistivity was continuously
10 measured using a DC current of 100 mA, with the samples maintained at a constant temperature
11 between 255 and 330 K for a few days.

12

13 3. Results

14 Figure 1 shows the time variation of resistivity (ρ) for Al-1.0%Mg2Si-0.2%Cu (noted as
15 Mg2Si02Cu, and similar notations in table I are used for samples) at 300 K. The horizontal axis
16 denotes the time (t) from SHTQ on a logarithmic scale. It is clear that ρ varies, firstly in an
17 increasing rate (concave shape), then later in a decreasing rate (convex shape) from around 10^3
18 minutes. Similar time variations are often observed in ternary and quaternary aluminum alloys but
19 not observed in pure aluminum or binary Al-Si/Al-Mg aluminum alloys (see supplement). Simple
20 estimations of the Fermi velocity (v_F) for conduction electrons of a pure aluminum and the relaxation
21 time (τ) for a typical ρ value observed for the present samples ($\rho \sim 4 \times 10^{-8} \Omega\text{m}$) yield $v_F \sim 2 \times 10^6$
22 m/s and $\tau \sim 5 \times 10^{-15}$ s, respectively, leading to the mean free path of approximately 10 nm. This
23 length has been often observed as a cluster size in ATP studies. Banhart et al. assigned four
24 clustering stages (stage I ~ IV) to the time variation of ρ in Al-Mg-Si alloys from PALS and ρ
25 measurements [22]. The time variation of ρ in Figure 1 is corresponding well to their assignment
26 for the stages I, II and III. For quantitative discussions, we adopted their method to evaluate the
27 stage transition time; the data points up to 250 minutes were fit with a linear function, those from
28 250 to 1100 minutes and from 1100 to 4000 minutes were fit with logarithmic functions: $\rho = \rho_0 + \rho^*$
29 $\log(t)$, (ρ^* is defined as a resistivity change coefficient in this paper). The arrows in Figure 1
30 indicate the intersections of the fitted functions, which are considered to be the stage boundaries.



1

2 Figure 1. Time dependence of electrical resistivity of an Al-1.0%Mg₂Si-0.20%Cu alloy at 300 K. The times
 3 that the electrical resistivity changes occur are marked by the arrows which were determined as the intersection
 4 points of the two least-square fits.
 5

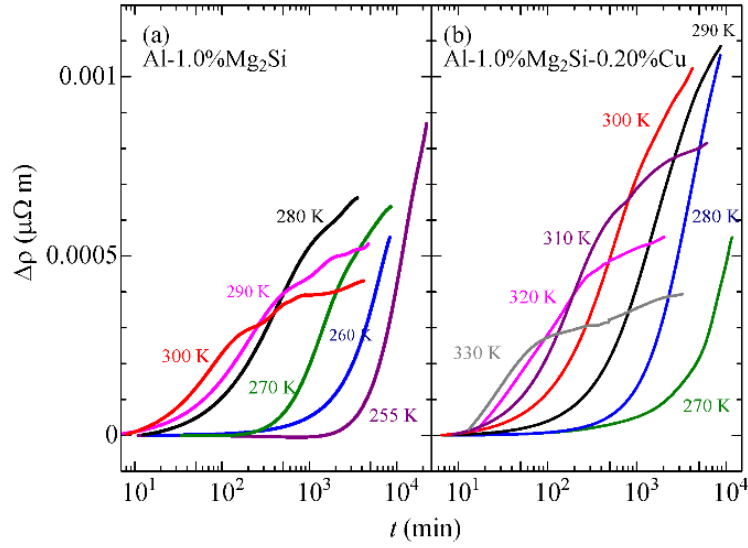
6

7

8 The time dependence of ρ for Al-1.0%Mg₂Si sample (noted as Mg₂Si) was measured in an
 9 isothermal condition with a temperature between 255 and 300 K. The results of the measurements
 10 are shown in Figure 2(a), in which the solid lines present the ρ changes ($\Delta\rho = \rho - \rho_0$, ρ_0 : an averaged
 11 value at the beginning) obtained by a least square fit of the data to a ninth degrees polynomial
 12 function. All lines increased with time. The stage transition time, at which ρ started to increase,
 13 was clearly delayed at the lower temperatures. Once ρ increased, however, the increasing rate of ρ
 14 was larger at the lower temperatures, and $\Delta\rho$ at 255 K seems to be maximum among the data lines in
 15 Figure 2(a). The $\Delta\rho$ vs. t for Mg₂Si_{0.2}Cu is presented in Figure 2(b). Over all appearances of the
 16 fitted lines are similar to those in Figure 2(a), except for the measuring temperature range which is
 17 approximately 30 K higher. A comparison of $\Delta\rho$ for Mg₂Si and Mg₂Si_{0.2}Cu at 280 K is given in
 18 Figure 3, in which it can be seen that the Cu addition clearly prolonged the stage transition time.
 19 The arrows in Figure 3 point the transition time from the stage I to II (t_{I-II}) deduced by the fitting as
 20 explained in Figure 1. There are a plenty of studies reporting similar Cu addition effect on the stage
 21 transition time [1, 25].
 22

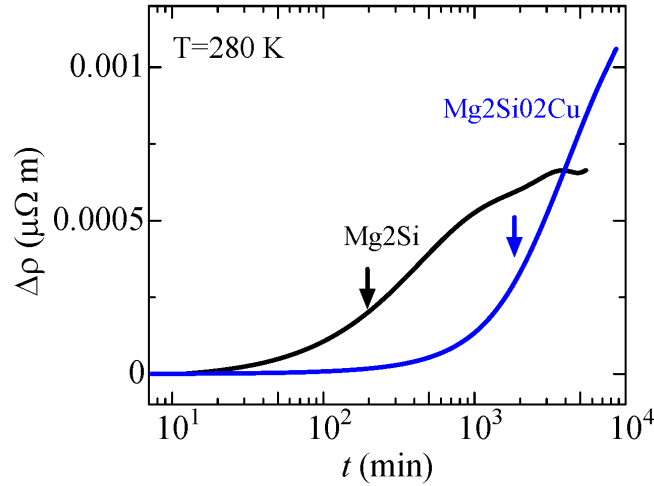
21

22



1
2
3
4
5

Figure 2. Time dependences of electrical resistivity changes of (a) Al-1.6%Mg₂Si alloy and (b) Al-1.0%Mg₂Si-0.20%Cu at a constant temperature between 255 and 330K.



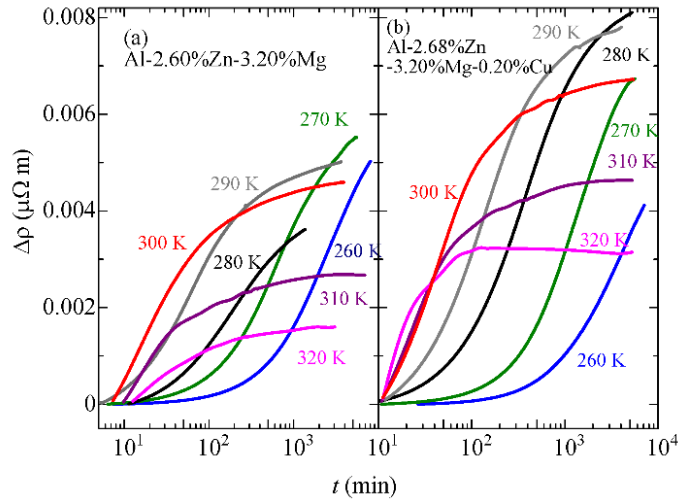
6
7
8
9
10

Figure 3. A comparison of the time dependences of electrical resistivity changes of Al-1.0%Mg₂Si and Al-1.0%Mg₂Si-0.20%Cu at 280 K.

11 Figures 4(a) and 4(b) show $\Delta\rho$ vs. t for ZnMg and ZnMg02Cu, respectively, at temperatures from
12 260 to 320 K. It is found that the same explanation as that given for Mg₂Si and Mg₂Si02Cu is
13 valid for ZnMg and ZnMg02Cu, indicating that t_{I-II} was delayed by the Cu addition. Figures 5(a)
14 and 5(b) show $\Delta\rho$ vs. t for MgGe and MgGe02Cu, respectively. It is worth mentioning that the
15 transition time from stage I to II for MgGe is noticeable even at 320 K in Figure 5(a), where
16 $\Delta\rho$ values at 320 K were reduced by half for drawing. Some of the ρ values decreased with time in
17 the early NA period. This different variation of $\Delta\rho$ vs. t between Al-Mg-Si(-Cu) and Al-Mg-Ge(-

1 Cu) is possibly ascribed to the different diffusivity of Si and Ge. Addition of Cu to MgGe further
 2 prolonged the stage transition time as seen in Figure 5(b). The magnitude of $\Delta\rho$ in MgGe is larger
 3 than that in MgGe0.2Cu for the later NA periods. This is opposite to those in Al-Mg-Si(-Cu) and
 4 Al-Zn-Mg(-Cu). The rather slow clustering behaviors of MgGe and MgGe0.2Cu made it difficult to
 5 measure the transition times from stage II to III due to the experimental limitations.

6



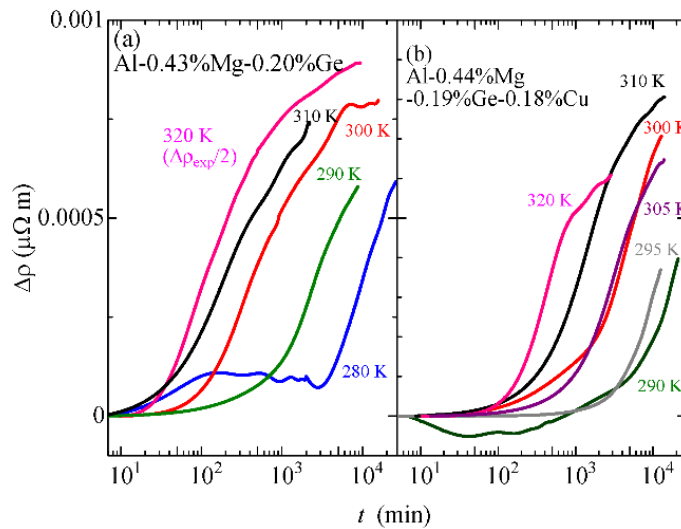
7

8

9 Figure 4. Time dependences of electrical resistivity changes of (a) Al-2.60%Zn-3.20%Mg and (b) Al-2.68%Zn-
 10 3.20%Mg-0.20%Cu at a constant temperature between 260 and 320K.

11

12



13

14

15 Figure 5. Time dependences of electrical resistivity changes of (a) Al-0.43%Mg-0.20%Ge and (b) Al-
 16 0.44%Mg-0.19%Ge-0.18%Cu at a constant temperature between 280 and 320K.

17

18

1 4. Discussions

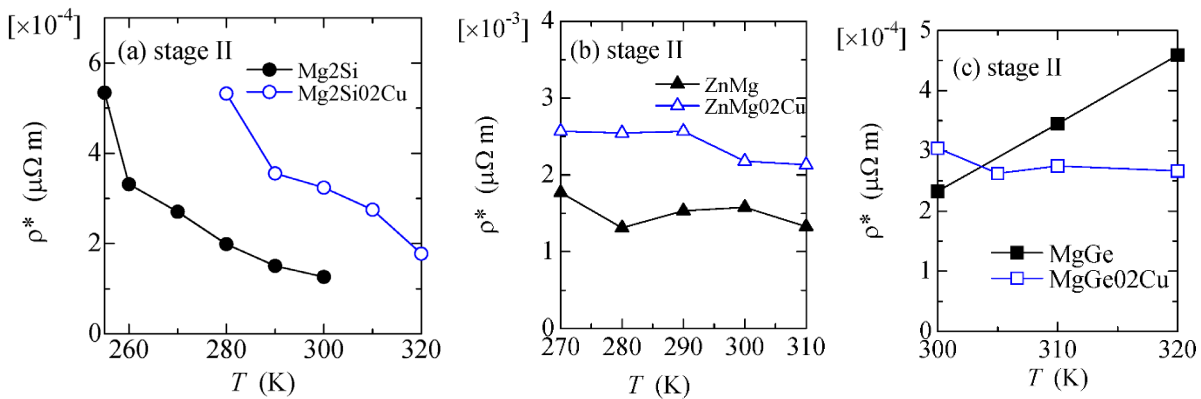
2 The time dependence of ρ in the present samples indicated that the Cu addition delayed the
 3 transition between stages I and II. In the initial clustering stage after SHTQ, quenched-in excess
 4 vacancies were caught by Cu atoms, so Si/Zn/Ge atoms were slow to make Si/Zn/Ge-vacancy pairs
 5 and complexes (stage I), consequently the Si/Zn/Ge-rich clustering (stage II) was prolonged.

6 Figure 6(a) shows the resistivity change coefficient (ρ^*) in stage II of Mg₂Si and Mg₂Si_{0.2}Cu
 7 calculated from the data in Figures 2(a) and 2(b). The ρ^* are larger at lower NA temperatures.
 8 This can be ascribed to the large number density of small sized clusters; the slow clustering due to a
 9 low temperature resulted in small Si-rich clusters [10, 25]. It is interesting that the ρ^* data points
 10 for Mg₂Si almost overlap with those of Mg₂Si_{0.2}Cu if they are shift toward the high temperature side
 11 by roughly 30 K. This finding implies that the added Cu atoms mainly interacted with vacancies,
 12 but did not significantly affect the Si-rich clustering in the stage II.

13 The ρ^* values for ZnMg and ZnMg_{0.2}Cu in Figure 6(b) are approximately an order of magnitude
 14 larger than those in Figure 6(a), due to the high Zn and Mg concentrations. The Cu addition
 15 definitely increased the ρ^* further, but the NA temperature dependence is unclear. The temperature
 16 dependences of ρ^* for Al-Mg-Ge(-Cu) in Figure 6(c) were found to be different from those for Al-
 17 Mg-Si(-Cu) and Al-Zn-Mg(-Cu) as the Cu addition did not always increase the ρ^* values. This
 18 result suggests that the clustering process in Al-Mg-Ge(-Cu) is different from those of Al-Mg-Si(-
 19 Cu) and Al-Zn-Mg(-Cu).

20

21

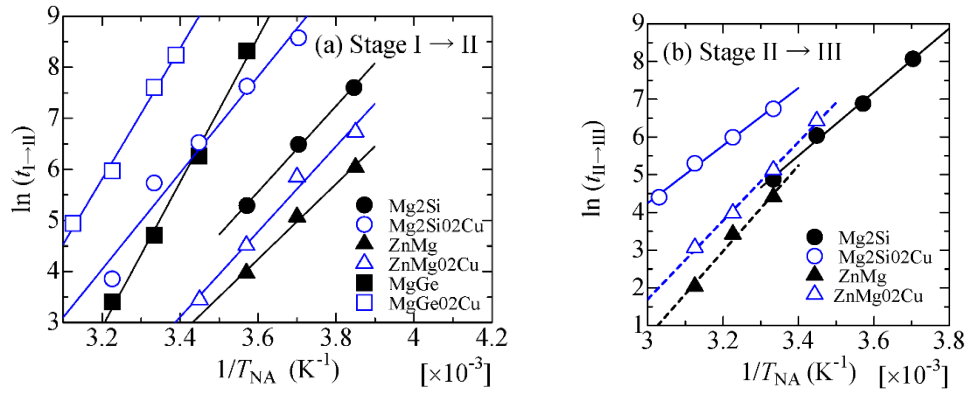


22

23 Figure 6. Comparison of the resistivity change coefficients of (a) Al-Mg-Si(-Cu), (b) Al-Zn-Mg(-Cu), and (c)
 24 Al-Mg-Ge(-Cu) samples in the clustering stage II.

25

26



1
2
3
4
5
6

Figure 7 Arrhenius plots for (a) Al-Mg-Si(-Cu), Al-Zn-Mg(-Cu), and Al-Mg-Ge(-Cu) using the transition times from stage I to II, and (b) Al-Mg-Si(-Cu) and Al-Zn-Mg(-Cu) using the transition times from stage II to III, and natural aging temperatures.

7 For more quantitative discussions about the Cu addition effect, the activation energies for cluster
8 formation (Q) were extracted from the stage transition times. Figures 7(a) (stage I - II) and 7(b)
9 (stage II - III) present Arrhenius plots of the logarithmic transition time against reciprocal
10 temperature of NA, $\ln(t) \sim Q/k_B T_{NA}$, based on the data in Figures 2 ~ 5, and the used values are listed
11 in table II. Least square fits of the data yield the activation energy, as drawn in Figures 8 and 9 for
12 the stage I - II and stage II - III, respectively. In Figure 8, the Q values were increased by the Cu
13 addition for Al-Mg-Si and Al-Zn-Mg in the transition between stage I and II, in which the Q value
14 obtained for Al-1.0%Mg2Si-0.35%Cu (noted as Mg2Si035Cu) in our previous study [26] is also
15 given. The Cu addition for Al-Mg-Ge, however, decreased the Q value. Further, in the stage
16 transition II - III, Cu additions in Al-Mg-Si and Al-Zn-Mg gave a small decrease in the Q values
17 (Fig. 9).

18

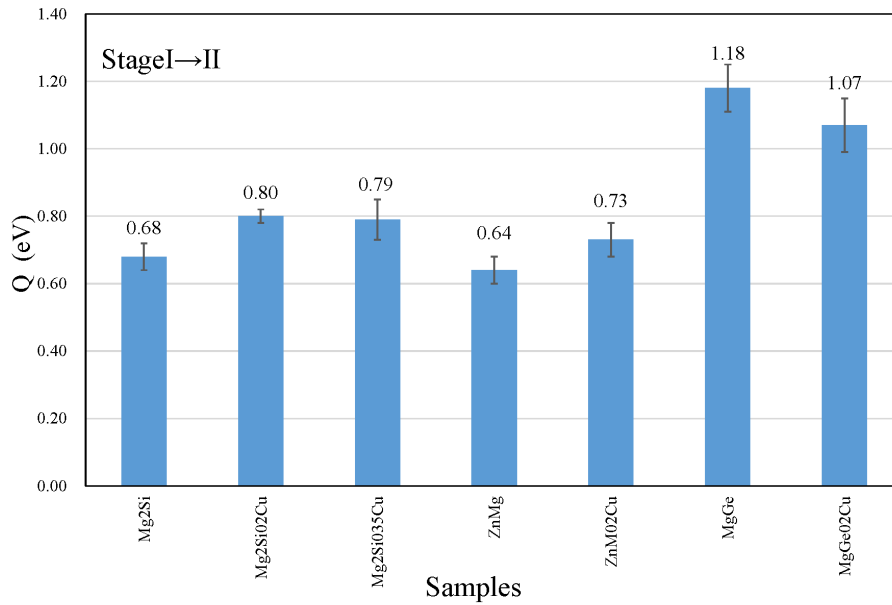


Figure 8 Activation clustering energy Q estimated from the Arrhenius plots in Figure 7(a).

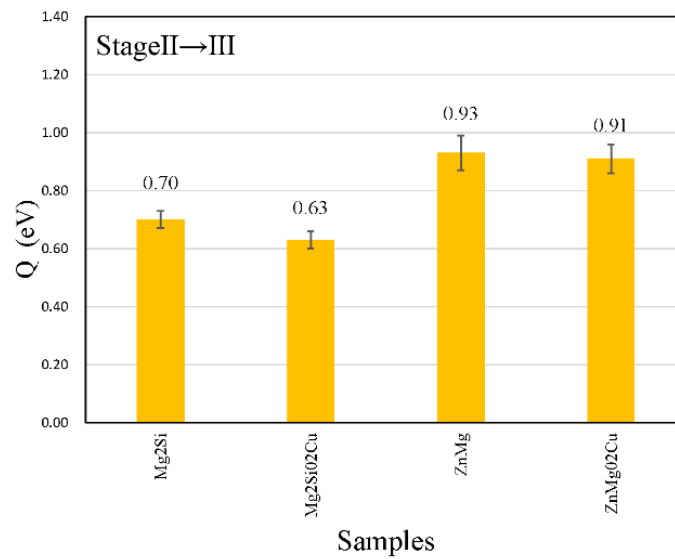


Figure 9 Activation clustering energy Q estimated from the Arrhenius plots in Figure 7(b).

The observed trends in the Q values by Cu additions most likely result from the vacancy behavior. Recent density functional theory calculations [25, 27-29] provide the solute-vacancy binding energies (E), for Si, Zn, Mg, Cu, and Ge atoms to be $E(\text{Si-V}) = 0.033$, $E(\text{Zn-V}) = 0.032$, $E(\text{Mg-V}) = 0.026$, $E(\text{Cu-V}) = 0.124$ and $E(\text{Ge-V}) = 0.053$ eV, respectively. As seen, the binding energy of Cu-vacancy is the largest among the present solute elements. Concerning the diffusivity (D), of the solutes, it is generally postulated that Si and Zn diffuse relatively fast with the aid of vacancies in aluminum, but Mg, Ge and Cu are slow to move at a natural aging temperature. A tentative

1 estimation using the parameters for the D values [30] yield $D(\text{Si}) \sim 5 \times 10^{-26}$, $D(\text{Zn}) \sim 7 \times 10^{-26}$,
2 $D(\text{Mg}) \sim 2 \times 10^{-26}$, $D(\text{Ge}) \sim 4 \times 10^{-26}$ and $D(\text{Cu}) \sim 2 \times 10^{-28}$ m^2/s in aluminum at 300 K, tells that the
3 $D(\text{Cu})$ value is two orders of magnitude smaller than the others. The solute elements need
4 vacancies to move and form clusters. Immediately after SHTQ, excess vacancies of approximately
5 100 ppm are considered to be present in aluminum alloys. This concentration is about one hundredth
6 of the solutes. A part of the vacancies will form solute-vacancy pairs, and others will be absorbed
7 in lattice imperfections such as grain boundaries, dislocation loops and impurities.

8 Based on this, Si-vacancy and Mg-vacancy pairs are produced first in Mg_2Si after SHTQ.
9 During NA in stage I, a mobile Si-vacancy pair will encounter other Si-vacancy pairs, starting to
10 form mobile Si complexes of a few Si atoms, releasing a part of vacancies, which leads to new
11 solute-vacancy pair formations. As the Si complexes grow larger in size and become clusters, the
12 vacancies will have difficulties to escape from the clusters [31]. Consequently, at the end of stage I,
13 a part of quenched-in vacancies is either trapped in the clusters or lost at imperfections. Since the
14 Mg-vacancy pairs move slowly, formation of Mg containing Si complexes proceeds in a slow rate.
15 Once stage I ends, however, the Mg-vacancy pairs play an important role to grow clusters and
16 release vacancies to transport solute atoms. This scenario can also be valid in the clustering process
17 for Al-Zn-Mg, since Zn-vacancy pairs move fast.

18 Since a Cu-vacancy pair has large binding energy and a relatively small diffusion rate, formations
19 of Si complexes in the Cu-added alloys during NA in stage I will proceed at a slower rate than in the
20 Cu-free alloys, due to the lower number density of Si(Zn)-vacancy pairs, leading to the larger $Q(\text{I-II})$
21 values. The DSC study by Chang et al. [32] reported that the $Q(\text{I-II})$ values mainly depended on the
22 Si concentrations in Al-Mg-Si alloys; the Mg concentration makes effect on the $Q(\text{II-III})$ [17]. The
23 activation energies for $\text{Mg}_2\text{Si}_02\text{Cu}$ and $\text{Mg}_2\text{Si}_035\text{Cu}$ are found to be almost the same within the
24 experimental errors. The electrical resistivity is mainly affected by cluster number density. The
25 APT work by Zandbergen et al. has reported the cluster number densities for Al-0.51%Mg-0.95%Si-
26 0.013%Cu, -0.06%Cu, and -0.34% Cu (at.%) annealed at 453 K for 30 min to be 6 ± 1 , 24 ± 2 , and
27 $37 \pm 4 \times 10^{22}/\text{m}^3$ [10]. The cluster number densities of the 0.06% and 0.34% Cu additions indicate a
28 saturation tendency. This experimental result implies that the cluster number density of
29 $\text{Mg}_2\text{Si}_035\text{Cu}$ was not much different from that of $\text{Mg}_2\text{Si}_02\text{Cu}$. At the end of stage I, a large
30 number density of small Si(Zn) clusters is expected. Since the distance between small solute
31 clusters in the Cu-added alloys is shorter than in the Cu-free ones, the Mg-vacancy pairs can
32 relatively easily encounter Si(Zn) clusters. Thus, the Si-Mg(-Cu) co-cluster formation is
33 accelerated, resulting in the smaller Q values from stage II to III for the Cu-added alloys.

34 For the Al-Mg-Ge(-Cu)alloys, we see that these three solutes have smaller diffusivity than those of

1 Si and Zn in NA, which can be responsible to the largest $Q(I-II)$ value of MgGe. The stage
2 transition time from stage I to II was definitely longer in MgGe02Cu, due to the Cu addition effect,
3 however, the deduced $Q(I-II)$ value is smaller than that in MgGe. This is opposite to the Al-Mg-
4 Si(-Cu) and Al-Zn-Mg(-Cu) cases. The APT study by Zheng et al. for Al-1.52%Cu-0.45%Mg-
5 0.076%Ge (at.%) revealed non-random distributions of Ge and Mg atoms in the as-quenched
6 condition, whereas Cu atoms remained largely in a random distribution. A possible explanation for
7 the Q values of Al-Mg-Ge(-Cu) is that, due to the slow clustering process, Ge- and Mg-vacancy
8 pairs/complex/cluster formations (stage I, II) and Ge-Mg co-cluster formations (stage III) proceed at
9 the same time during the long first stage. (In this sense, the first stages observed in Al-Mg-Ge(-Cu)
10 are perhaps different from those in Al-Mg-Si(-Cu) and Al-Zn-Mg(-Cu), but we leave it as stage I for
11 consistency) Since the total solute concentration of MgGe02Cu is larger than that of MgGe, we
12 expect a larger number of solute-vacancy pairs in MgGe02Cu in the early stage of NA. The larger
13 number of solute-vacancy pairs makes the distance between the pairs shorter and easier to form
14 complexes/clusters, leading to the smaller $Q(I-II)$ value in MgGe02Cu.

15

16 5. Conclusion

17 Time-dependent resistivity measurements of Al-Mg-Si(-Cu), Al-Zn-Mg(-Cu) and Al-Mg-Ge(-Cu)
18 alloys have been carried out at constant temperatures between 255 and 320 K. The effect of Cu
19 additions on the stage transition time has been evaluated, which enable quantitative discussions about
20 cluster activation energies. From the present study three conclusions can be drawn;

21 1. Cu additions in Al-1.0%Mg₂Si, Al-2.68%Zn-3.20%Mg, and Al-0.44%Mg-0.19%Ge prolonged the
22 stage transition time from stage I to II, due to the strong binding energy between Cu and vacancy,
23 resulting in fewer vacancies available for solute atoms to diffuse in aluminum.

24 2. The Cu addition was found to increase the activation energy from stage I to II for Al-1.0%Mg₂Si
25 and Al-2.68%Zn-3.20%Mg, but decrease the activation energy from stage II to III. The slow
26 clustering in stage I led to a large number density of small sized Si or Zn clusters, which accelerate
27 the Si(Zn)-Mg co-clustering in stage II.

28 3. It was found that the Cu addition to Al-0.44%Mg-0.19%Ge prolonged the stage transition time of
29 the first stage, but decreased the activation energy in the same stage, in which a combined clustering
30 process of solute-vacancy pair/complex and solute-cluster formations can explain this tendency.

31

32

33 Acknowledgments

34 This study has been supported by the funds from Center for Advanced Materials Research and

1 International Collaboration, University of Toyama, The Norwegian-Japanese Aluminium alloy
2 Research and Education Collaboration (INTPART), project number 249698, and The Japan Institute
3 of Light Metals.

4
5 References:

- 6 [1] M. Werinos, H. Antrekowitsch, T. Ebner, R. Prillhofer, P.J. Uggowitzer, and S. Pogatscher : *Mater. Des.*,
7 2016, vol.107, pp. 257-268.
- 8 [2] S.K. Maloney, K Hono, I.J. Polmear, and S.P. Ringer: *Micron*,2001, vol. 32, pp. 741-747
- 9 [3] Y. Weng, Z. Jia, L. Ding, Y. Pan, Y. Liu, and Q. Liu : *J. Alloy. Compd.*, 2017, vol. 695, pp. 2444-2452.
- 10 [4] Q. Xiao, H. Liu, D. Yi, D. Yin, Y. Chen, Y. Zhang, and B. Wang : *J. Alloy. Compd.*, 2017, vol. 695, pp.
11 1005-1013.
- 12 [5] K. Matsuda, A. Kawai, K. Watanabe, S. Lee, C. D. Marioara, S. Wenner, K. Nishimura, T. Matsuzaki, N.
13 Nunomura, T. Sato, R. Holmestad, and S. Ikeno: *Mater. Trans.* 2017, vol. 58, pp. 167-175
- 14 [6] G.Tao, C.Liu, J.Chen, Y.Lai, P.Ma and L.Liu : *Mater. Sci. Eng., A*, 2015, vol. 642, pp. 241-248.
- 15 [7] M. Murayama and K. Hono: *Acta Mater.*, 1999, vol. 47, pp. 1537-1548.
- 16 [8] G. Sha and A. Cerezo: *Acta Mater.*, 2004, vol. 52, pp. 4503-4516.
- 17 [9] A. Serizawa, S. Hirosawa, and T. Sato: *Metall. Mater. Trans., A*, 2008, vol. 39, pp. 243-251.
- 18 [10] M. W. Zandbergen, A. Cerezo, and G. D. W. Smith: *Acta Mater.*, 2015, vol. 101, pp. 149-158.
- 19 [11] Y. Aruga, M. Kozuka, Y. Takaki, and T. Sato: *Scr. Mater.*, 2016, vol. 116, pp. 82-86.
- 20 [12] Z. Jia L. Ding L. Cao, R. Sanders, S. Li, and Q. Liu: *Metall. Mater. Trans., A*, 2017, vol. 48, pp. 459-473.
- 21 [13] C.S.T. Chang and J. Banhart : *Metall. Mater. Trans., A*, 2011, vol. 42, pp. 1960-1964.
- 22 [14] J.H. Kim, E. Kobayashi, and T. Sato : *Mater. Trans.*, 2011, vol. 52, pp. 906-913.
- 23 [15] L. Ding, Z. Jia, Y. Liu, Y. Weng, and Q. Liu : *J. Alloy. Compd.*, 2016, vol. 688, pp. 362-367.
- 24 [16] M. Liu, B. Klobes, and J. Banhart: *Mater. Sci.*, 2016, vol. 51, pp. 7754-7767.
- 25 [17] J. Banhart, M.D. H.Lay, C.S.T. Chang, and A.J. Hill: *Phys. Rev. B*, 2011, vol. 83, pp. 014101-014113.
- 26 [18] M.D. H. Lay, H.S. Zurob, C.R. Hutchinson, T.J. Hill, and A.J. Hill : *Metall. Mater. Trans., A*, 2012, vol.
27 43, pp. 4507-4513.
- 28 [19] S. Wenner, R. Holmestad, K. Matsuda, K. Nishimura, T. Matsuzaki, D. Tomono, F.L. Platt, and C.D.
29 Marioara : *Phys. Rev. B*, 2012, vol. 86, pp. 014201-014207.
- 30 [20] S. Wenner, K. Nishimura, K. Matsuda, T. Matsuzaki, D. Tomono, F.L. Platt, C.D. Marioara, and R.
31 Holmestad : *Acta Mater.*, 2013, vol. 61, pp. 6082-6092.
- 32 [21] K. Nishimura, K. Matsuda, R. Komaki, N. Nunomura, S. Wenner, R. Holmestad, T. Matsuzaki, I. Watanabe,
33 F.L. Pratt, and C.D. Marioara: *J. Phys. Conf. Ser.*, 2014, vol. 551, 012031.
- 34 [22] J. Banhart, C.S.T. Chang, Z. Liang, N. Wanderka, M.D. H.Lay, and A.J. Hill: *Adv. Eng. Mater.*, 2010, vol.
35 12, pp. 559-571.
- 36 [23] H. Seyedrezai, D. Grebennikov, P. Mascher, and H. S. Zurob: *Mater. Sci. Eng.*, 2009, vol. 525, pp. 186-
37 191.
- 38 [24] J.H. Kim, H. Tezuka, E. Kobayashi, and T. Sato : *Kor. J.Mater. Res.*, 2012, vol. 22, pp. 329-334.

- 1 [25] M. Liu and J. Banhart: *Mater. Sci. Eng. A*, 2016, vol. 658, pp. 238-245.
- 2 [26] D. Hatakeyama, K. Nishimura, T. Namiki, K. Matsuda, N. Nunomura and T. Matsuzaki : Japan Institute
3 of Light Metals, 2017, vol. 67, pp. 168-172. (in Japanese)
- 4 [27] P. Lang, Y.V. Shan, and E. Kozeschnik : *Mater. Sci. Forum*, 2014, vols.794-796, pp. 963-970.
- 5 [28] P. Lang, T. Weisz, M.R. Ahmadi, E. Povoden-Karadeniz, A. Falahati, and E. Kozeschnik : *Adv. Mater.*
6 *Res.*, 2014, vol. 922, pp. 406-411.
- 7 [29] C. Worverton : *Acta Mater.*, 2007, vol. 55, pp. 5867-5872.
- 8 [30] Y. Du, Y. A. Chang, B. Huang, W. Gong, Z. Jin, H. Xu, Z. Yuan, Y. Liu, Y. He, F.-Y. Xie: *Mater. Sci.*
9 *Eng. A* 2003, vol. 363, pp. 140-151
- 10 [31] H.S. Zurob and H. Seyedrezai: *Scr. Mater.*, 2009, vol. 61, pp. 141-144.
- 11 [32] C. S. T Chang, Z. Liang, E. Schmidt, and J. Banhart: *Int. J. Mat Res.* 2012, vol. 103, pp. 955-961

12
13
14
15
16
17
18
19
20
21
22
23
24
25
26
27
28
29
30
31
32
33
34
35
36
37
38

Table1 Sample composition of studied alloys, sample notation labels, and solution heat treatment (SHT) temperature.

Sample composition [at.%]	Notation	SHT temp. [K]
Al-1.0%Mg2Si	Mg2Si	
Al-1.0%Mg2Si-0.20%Cu	Mg2Si02Cu	848
Al-2.60%Zn-3.20Mg	ZnMg	753
Al-2.68%Zn-3.20%Mg-0.20%Cu	ZnMg02Cu	
Al-0.43%Mg-0.20%Ge	MgGe	873
Al-0.44%Mg-0.19%Ge-0.18%Cu	MgGe02Cu	

Table2 Transition times between stages I - II, and stages II - III.

n.a. temp [K]	260	270	280	290	295	300	310	320
alloy	t [min] Stage I - II							
Mg2Si	2000	658	198					
Mg2Si02Cu		5099	1953	682		339	48	
ZnMg	420	159	53					
ZnMg02Cu	837	347	91	32				
MgGe			4109	524		111	30	
MgGe02Cu					3793	2005	393	140

n.a. temp [K]	270	280	290	300	310	320	330
alloy	t [min] Stage II - III						
Mg2Si	3197	975	419	132			
Mg2Si02Cu				850	400	201	82
ZnMg				82	31	10	
ZnMg02Cu			618	168	54	22	

1 List of figure captions

2 Figure 1. Time dependence of electrical resistivity of an Al-1.0%Mg₂Si-0.20%Cu alloy at 300 K. The times
3 that the electrical resistivity changes occur are marked by the arrows which were determined as the intersection
4 points of the two least-square fits.

5

6 Figure 2. Time dependences of electrical resistivity changes of (a) Al-1.6%Mg₂Si alloy and (b) Al-1.0%Mg₂Si-
7 0.20%Cu at a constant temperature between 255 and 330K.

8

9 Figure 3. A comparison of the time dependences of electrical resistivity changes of Al-1.0%Mg₂Si and Al-
10 1.0%Mg₂Si-0.20%Cu at 280 K.

11

12 Figure 4. Time dependences of electrical resistivity changes of (a) Al-2.60%Zn-3.20%Mg and (b) Al-2.68%Zn-
13 3.20%Mg-0.20%Cu at a constant temperature between 260 and 320K.

14

15 Figure 5. Time dependencies of electrical resistivity changes of (a) Al-0.43%Mg-0.20%Ge and (b) Al-
16 0.44%Mg-0.19%Ge-0.18%Cu at a constant temperature between 280 and 320K.

17

18 Figure 6. Comparison of the resistivity change coefficients of (a) Al-Mg-Si(-Cu), (b) Al-Zn-Mg(-Cu), and (c)
19 Al-Mg-Ge(-Cu) samples in the clustering stage II.

20

21 Figure 7 Arrhenius plots for (a) Al-Mg-Si(-Cu), Al-Zn-Mg(-Cu), and Al-Mg-Ge(-Cu) using the transition
22 times from stage I to II, and (b) Al-Mg-Si(-Cu) and Al-Zn-Mg(-Cu) using the transition times from stage II to
23 III, and natural aging temperatures.

24

25 Figure 8 Activation clustering energy Q estimated from the Arrhenius plots in Figure 7(a).

26

27 Figure 9 Activation clustering energy Q estimated from the Arrhenius plots in Figure 7(b).

28